



Cardiac segments dosimetric benefit from deep inspiration breath hold technique for left-sided breast cancer radiotherapy

Elisabet González-del Portillo¹, Jorge Hernández Hernández-Rodríguez², Enrique Tenllado-Baena², Álvaro Fernández-Lara², Orlanda Alonso-Rodríguez³, Ángela Matías-Pérez³, Cristina Cigarral-García³, Graciela García-Álvarez³, Luis A. Pérez-Romasanta⁴

¹Department of Radiation Oncology, La Paz University Hospital, Madrid, Spain

²Department of Radiation Physics, Salamanca University Hospital, Salamanca, Spain

³Department of Radiation Oncology, Salamanca University Hospital, Salamanca, Spain

⁴Department of Radiation Oncology, Salamanca University Hospital, IBSAL, Salamanca, Spain

ABSTRACT

Background: The objective was to compare dosimetry in left-sided breast cancer (LSBC) patients receiving deep inspiration breath hold (DIBH) radiotherapy (RT) with free-breathing (FB) treatment plans.

Materials and methods: Voluntary DIBH with a spirometer-based video-assisted system and CT-simulation were performed under FB and DIBH conditions on 40 LSBC patients, segmented according Duane's atlas. IMRT plans kept the same dosimetric goals on FB and DIBH conditions. Target, lungs and heart volumes were measured. Planning target volume (PTV) dose distribution, organs at risk (OARs) dose/volume parameters, including cardiac substructures, were calculated.

Results: Lungs and left-lung volumes increased in DIBH conditions ($\Delta V = 1637.8 \text{ ml} \pm 555.3$ and $783.5 \text{ ml} \pm 286.4$, respectively). Heart volume slightly decreased in apnea ($p = 0.04$), but target volumes, CTV and PTV were similar in FB or DIBH plans. PTV dose coverage was similar irrespective of respiratory conditions (median $D50\% = 41.1 \text{ Gy}$ vs 41.0 Gy , $p = 0.665$; $V95\% = 96.9\%$ vs. 97%). Mean dose for the whole heart (MHD), left ventricle (LV), and LV segments were significantly reduced in DIBH plans. $V20$ values for heart subvolumes were significantly different only for those that received considerable doses (apical and anterior). DIBH plans provided significantly smaller doses (D_{\max} , $D2\%$, and $V20$) to the LAD artery.

Conclusion: Important dosimetric improvements can be achieved with DIBH technique for LSBC patients, reducing the dose to the LAD artery and heart, particularly to the segments closer to the chest wall. Apical/anterior LV segments, should be considered as separate organ at risk in breast RT.

Key words: left sided breast cancer; radiation therapy; deep inspiration breath hold

Rep Pract Oncol Radiother 2024;29(1):21–29

Introduction

Breast cancer is the most common cancer in women. Early invasive breast cancer is limited to

the breast and ipsilateral axilla. The primary treatment of early invasive breast cancer is usually surgical excision followed frequently by risk adapted adjuvant treatments, including radiation therapy,

Address for correspondence: Luis A. Pérez-Romasanta, Oncología Radioterápica, Hospital Universitario de Salamanca, Instituto de Investigaciones Biomédicas de Salamanca (IBSAL), 37007 Salamanca, Spain; e-mail: lapromasanta@saludcastillayleon.es

This article is available in open access under Creative Common Attribution-Non-Commercial-No Derivatives 4.0 International (CC BY-NC-ND 4.0) license, allowing to download articles and share them with others as long as they credit the authors and the publisher, but without permission to change them in any way or use them commercially

hormone therapy, biological therapies, or chemotherapy. Whatever treatment is used, the reduction of chronic toxicity in patients with breast cancer becomes of the paramount importance due to the continuous improvement of the vital prognosis.

Radiation therapy (RT) to the left breast usually involves incidental irradiation of the heart and left lung. Cardiac irradiation increases the risk of radiation-induced cardiac alterations, including major coronary events, proportional to dose with a relative increase of 7.4% (95% confidence interval, 2.9 to 14.5) per Gy of mean heart dose (MHD) received [1]. There is no cardiac dose threshold below which radiation therapy is safe, so the cardiac dose should be kept as low as possible [2–4]. It is still unknown which dosimetric parameter is best related to specific cardiac toxicities, whether it is the MHD, the maximum doses (D_{max}) to the coronary arteries, or the dose distribution in a particular cardiac substructure. In addition, RT can cause lung lesions, such as reduction of lung function, radiological alterations, radiation pneumonitis, fibrosis and radiation induced tumors [5]. The combination of lung and heart damage could cooperate for a net cardiorespiratory functional deterioration after irradiation mainly in the long term.

Deep inspiration breath-hold (DIBH) is a method of limiting radiation exposure to the lung and heart in patients receiving radiation therapy to the left breast [4]. The basis of the technique simply involves the movement of organs at risk (OARs) away from the treatment area by stopping respiratory movement at the optimal stage of the respiratory cycle. Numerous studies have shown that the DIBH technique allows for heart preservation during the RT of the left breast, reducing the MHD by 26.2–75.0% compared to standard free-breathing (FB) and leaving the absolute MHD between 0.7–5.0 Gy [6, 7]. The use of modern RT techniques with dose intensity modulation of the beam (IMRT) combined with DIBH can achieve even greater reductions in MHD [8]. Left lung dose reductions have also been observed with the DIBH technique [6, 7]. Other additional advantages as derived from the elimination of respiratory movement during RT with the DIBH technique have been described such as the reduction of the margins necessary to compensate for the movement

of the target volume (the breast or chest wall) and the greater precision in the administration of the planned dose [9].

Quantifying radiation dose to cardiac substructures is important for research on the etiology and prevention of complications following RT [10]; however, segmentation of substructures is challenging. Cardiac atlases based on computed tomography (CT) images have been developed for the radiation therapy field, resulting in a variable number of substructures [11–19]. Deep-learning, machine-learning, knowledge-based, and artificial-intelligence methods can help reducing the variability inherent to the manual contouring of so many substructures [20].

The main purposes of this work are to quantify the magnitude of DIBH dosimetric benefits and identify which cardiac substructures experience a significant dose reduction in patients with diagnosis of early left-sided breast cancer who were treated with RT under DIBH conditions.

Materials and methods

Patients

Forty consecutive patients with left-sided breast cancer were included if they were in a good performance status [Eastern Cooperative Oncology Group (ECOG) 0–1], they were able to maintain DIBH for more than 20 seconds, and able to follow the visual instructions of the respiratory synchronization system. Conservative treatments as well as post-mastectomy treatments were included, with or without RT to the axillary lymph node levels 1–4.

Deep inspiration breath hold technique

The spirometric breath-hold system SDX® (Dyn'R, Toulouse, France) consists of blocking voluntarily the patient's breathing in inspiration, during acquisition, and irradiation. The DIBH technique involved patient training immediately prior to CT simulation. The training or preparation phase is required to define a comfortable degree of deep inspiration for the patient. This level usually corresponds to 85% of the patient's maximum inspiration with a 10% tolerated variability.

Immobilization and image acquisition

All patients were simulated and treated on a breast-board in a supine position with both hands

above the head. Two CT acquisitions were performed for each patient: the first CT acquisition was performed with the DIBH device and a final acquisition was performed in FB. An injection of contrast agent was performed during DIBH acquisition to facilitate delineation of target volumes.

Contouring

Target volumes were defined according to International Commission on Radiation Units and Measurements general recommendations, following the European Society for Radiotherapy and Oncology (ESTRO) specific guidelines for elective radiation therapy of early stage breast cancer [21]. The defined OARs were the left and right lung, total lung volume, the heart and the heart substructures according Duane's cardiac contouring atlas [16]. From the 15 cardiac segments included in Duane's atlas, the following structures were contoured for this study: left anterior descendant (LAD) artery, whole heart, left and right ventricles, apical, anterior, septal, lateral, and inferior left ventricle (LV) segments.

Treatment planning and dosimetric data extraction

For each patient, tangential fields and sub-fields plans on the FB and DIBH scans were developed using segmental IMRT. The aim of the plans was to cover $\geq 95\%$ of the planning target volume (PTV) with $\geq 95\%$ of the prescription dose. Two fractionation schedules were used: 50 Gy/25 fractions in 5 weeks (Conv) and 40 Gy/15 fractions hypofractionated schedule within 3 weeks (Hypo). Dose volume histograms (DVH) were exported from Eclipse (Varian Medical Systems) in text format. Automatic data extraction from DVH was scripted in MATLAB® (The MathWorks Inc.). Relevant dosimetric parameters from targets and OARs were tabulated for posterior statistical analysis.

Treatment administration

The daily reproducibility was assessed by electronic portal acquisitions according to a No-Action Level (NAL) protocol.

Endpoints and statistical analysis

To investigate the dose homogeneity of target coverage, the PTV median dose (D50%) and PTV

V95% were calculated. The relative change when using DIBH as opposed to FB was compared for standard defined parameters: MHD, mean ventricles dose, V10 and V20 in the heart and ventricles, mean dose and V20 for several heart subvolumes, Dmax, D2% and V20 for LAD artery, and total lung and left lung V20, V10 and V5.

To test if an individual group of data (from FB or DIBH) comes from a standard normal distribution, the Kolmogorov-Smirnov (K-S) test was conducted. The Lilliefors test, a less restrictive test of normality, was also conducted. The significance level is established at 0.05 in both cases.

To evaluate FB vs. DIBH (paired data populations), non-parametric tests for continuous variables were used. The selected test for comparison was non-parametric Wilcoxon Signed Rank Test. Assuming data from the differences between the two observations comes from a symmetric and continuous distribution around its median value, the null hypotheses tests if this distribution has zero median. The significance level chosen is 0.05.

Results

Normality tests (Kolmogorov-Smirnoff and Lilliefors tests) showed that structure volumes followed a normal distribution but dose and dose-volume histogram (HDV) derived parameters did not. Therefore, mean values were used to describe the organ volumes and median values were used to describe the dose related parameters.

Patient characteristics

The patient and tumor characteristics are displayed in Table 1.

Target volumes and doses

The clinical target volume (CTV) and PTV volumes under FB or DIBH conditions were similar: 733 ± 337 mL vs. 729 ± 336 mL ($p = 0.815$) for CTVs and 917 ± 385 mL vs. 913 ± 385 mL ($p = 0.861$) for PTVs. PTV dose coverage was similar disrespect of respiratory conditions. For hypofractionated regime, median PTV-D_{50%} was 41.1 Gy under FB conditions versus 41.0 under DIBH conditions, $p = 0.665$. For conventional fractionation regime, median D50% was 51.3 under FB conditions versus 51.4 under DIBH conditions, $p = 1.0$. Regarding

Table 1. Patient and tumor characteristics

Characteristic	Category	Mean ± SD*	n (%)**
Age*		52.8 ± 8.1	
BMI*		25.2 ± 4.6	
Tumor location**	Inner quadrants		10 (25%)
	Outer quadrants		21 (52.5%)
	Periareolar and interquadrants		9 (22.5%)
Stage T**	cis		2 (5.0%)
	pT1a		1 (2.5%)
	pT1b		11 (27.5%)
	pT1c ¹		17 (42.5%)
	pT2 ²		9 (22.5%)
Stage N**	pN0		33 (82.5%)
	pNmic		4 (10.0%)
	pN1		1 (2.5%)
	pN2a		1 (2.5%)
	pNx		1 (2.5%)
Stage group**	cis		2 (5.0%)
	IA		24 (60.0%)
	IB		4 (10.0%)
	IIA		8 (20.0%)
	IIB		1 (2.5%)
	IIIA		1 (2.5%)
Supraclavicular field**	Yes		2 (5.0%)
	No		38 (95%)
Fractionation**	Conv		3 (7.5%)
	Hypo		37 (92.5%)

*Results presented as mean ± standard deviation (SD); **Results presented as Number and Percentage; ¹Sixteen patients pT1c and one patient cT1c converted into pT0 after neoadjuvant treatment; ²Six patients pT2 and three patients cT2 converted into ypT0 (one patient) or ypT1b (two patients); BMI — body mass index

PTV- $V_{95\%}$, the median values were almost identical: 97% for FB and 96.9% for DIBH conditions.

Lung volumes and doses

The mean total lung and left lung volumes under FB versus DIBH conditions were 2954 ± 578 mL vs. 4592 ± 740 mL ($p < 0.001$) and 1368 ± 311 mL vs. 2141 ± 372 mL ($p < 0.001$), respectively. Median total lung mean dose and median total lung V20 values under FB versus DIBH conditions were 3.5 Gy versus 3.3 Gy ($p = 0.06$) and 5.9% vs. 5.2% ($p = 0.33$). Three dose levels of 20Gy, 10 Gy, and 5 Gy were established to determine the fractional volumes V20, V10 and V5 for the left lung. The median values under FB versus DIBH conditions were, for V20 13.1% vs. 11–4% ($p = 0.008$); for V10, 18.6% vs. 17.1% ($p = 0.003$); and for V5, 28.2%

vs. 26.2% ($p < 0.001$). All lung volumes and doses are described in Table 2.

Left anterior descending artery doses

The radiation dose to the LAD artery was reduced under DIBH conditions: median Dmax, median $D_{2\%}$, and median $V_{20\%}$ were 39.0 Gy, 37.2 Gy, and 44.2% for FB conditions versus 27.6 Gy, 21.2 Gy, and 3.1% for DIBH conditions ($p < 0.001$ for all comparisons) (Tab. 3).

Heart volumes and doses

Mean whole heart volume resulted in slightly smaller DIBH (475.7 ± 104.7 mL vs. 503.3 ± 129.2 mL; $p = 0.04$). The median MHD was 2.9 Gy under FB conditions versus 1.7 Gy under DIBH conditions ($p < 0.001$) (Tab. 2). Dose-volume

Table 2. Lung volume change, dose, and dose-volume histogram (DVH) selected parameters in deep inspiration breath-hold (DIBH) or free-breathing (FB) conditions

Structure	Parameter	DIBH	Range	FB	Range	p
Lungs	D _{mean} [Gy]	3.3 ± 0.7	5.3–2.0	3.7 ± 0.9	6.8–2.1	0.06
	D _{median} [Gy]	3.3		3.5		
	Mean V ₂₀ (%)	5.6 ± 1.6	9.5–2.9	6.1 ± 2.1	12.7–2.6	0.33
	Median V ₂₀ (%)	5.2		5.9		
	Mean Δ-Volume [cm ³]	+1637.8 ± 555.3			3389.3–664.1	< 0.001
	Median Δ-Volume [cm ³]	+1632.8				
Left lung	Mean V ₂₀ (%)	12.1 ± 3.4	20.4–6.2	13.3 ± 4.8	27.6–7.2	0.008
	Median V ₂₀ (%)	11.4		13.1		
	Mean V ₁₀ (%)	17.7 ± 3.9	28.3–9.9	19.0 ± 6.0	37.3–12.4	0.003
	Median V ₁₀ (%)	17.1		18.6		
	Mean V ₅ (%)	27.2 ± 5.1	38.7–16.6	29.2 ± 8.1	49.1–19.9	< 0.001
	Median V ₅ (%)	26.8		28.2		
	Mean Δ-Volume [cm ³]	+783.5 ± 286.4			1,705.2–217.6	< 0.001
	Median Δ-Volume [cm ³]	+772.0				

Δ-Volume — volume change between FB and DIBH conditions

Table 3. D_{mean} and dose-volume histogram (DVH) parameters for heart structures. Mean ± standard deviation (Median) for hypofractionated and conventionally fractionated regimes

	Parameter	DIBH	Range	FB	Range	p
LAD artery	D _{max} [Gy]	24.4 ± 14.2 (27.6)	50.5–3.1	36.2 ± 11.1 (39.0)	51.4–6.0	< 0.001
	D _{2%} [Gy]	21.0 ± 14.2 (21.2)	49.4–2.7	33.4 ± 12.1 (37.9)	50.7–4.9	< 0.001
	V ₂₀ (%)	17.1 ± 25.8 (25.8)	93.2–0.0	42.3 ± 30.9 (44.2)	95.7–0.0	< 0.001
Heart	D _{mean} [Gy]	1.9 ± 1.0 (1.7)	4.5–0.6	3.1 ± 1.4 (2.9)	7.7–0.8	< 0.001
	V ₂₀ (%)	1.2 ± 1.8 (0.5)	7.4–0.0	3.2 ± 2.8 (2.3)	13.8–0.0	< 0.001
	V ₁₀ (%)	2.1 ± 2.6 (1.1)	11.1–0.0	4.9 ± 3.8 (3.9)	19.8–0.0	< 0.001
LV	D _{mean} [Gy]	2.5 ± 1.5 (2.1)	7.6–0.9	4.5 ± 2.4 (3.8)	12.7–1.2	< 0.001
	V ₂₀ (%)	1.7 ± 3.1 (0.3)	7.4–0.0	5.3 ± 5.4 (4.5)	24.6–0.0	< 0.001
Right ventricle	D _{mean} [Gy]	1.4 ± 0.6 (1.2)	3.4–0.6	2.1 ± 1.2 (1.7)	5.6–0.9	< 0.001
	V ₂₀ (%)	0.1 ± 0.5 (0.0)	3.3–0.0	0.7 ± 1.5 (0.0)	6.3–0.0	–
LV Apical segment	D _{mean} [Gy]	5.5 ± 4.7 (4.0)	21.7–1.5	13.0 ± 8.0 (11.3)	38.0–2.3	< 0.001
	V ₂₀ (%)	6.9 ± 13.2 (0.3)	56.0 - 0.0	25.1 ± 23.8 (17.5)	94.9–0.0	< 0.001
LV Anterior segment	D _{mean} [Gy]	4.6 ± 4.2 (3.7)	20.9–1.2	7.9 ± 7.1 (5.9)	36.0–1.9	< 0.001
	V ₂₀ (%)	3.6 ± 13.0 (0.0)	65.2–0.0	10.5 ± 19.3 (0.9)	85.9–0.0	< 0.001
LV Septal segment	D _{mean} [Gy]	1.6 ± 0.9 (1.4)	3.9–0.6	2.4 ± 1.4 (2.0)	7.7–0.9	< 0.001
	V ₂₀ (%)	0.0 ± 0.1 (0.0)	0.5–0.0	0.3 ± 1.6 (0.0)	9.9–0.0	–
LV Lateral segment	D _{mean} [Gy]	1.9 ± 1.2 (1.6)	6.2–0.8	3.2 ± 2.6 (2.5)	15.4–0.8	< 0.001
	V ₂₀ (%)	0.0 ± 0.2 (0.0)	1.0–0.0	1.2 ± 5.3 (0.0)	30.9–0.0	–
LV Inferior segment	D _{mean} [Gy]	0.8 ± 0.7 (0.6)	3.6–0.3	1.3 ± 1.0 (0.9)	4.4–0.5	< 0.001
	V ₂₀ (%)	0.0 ± 0.0 (0.0)	0.0–0.0	0.0 ± 0.0 (0.0)	0.0–0.0	–

DIBH — deep inspiration breath-hold; FB — free-breathing; LAD — left anterior descending; LV — left ventricle

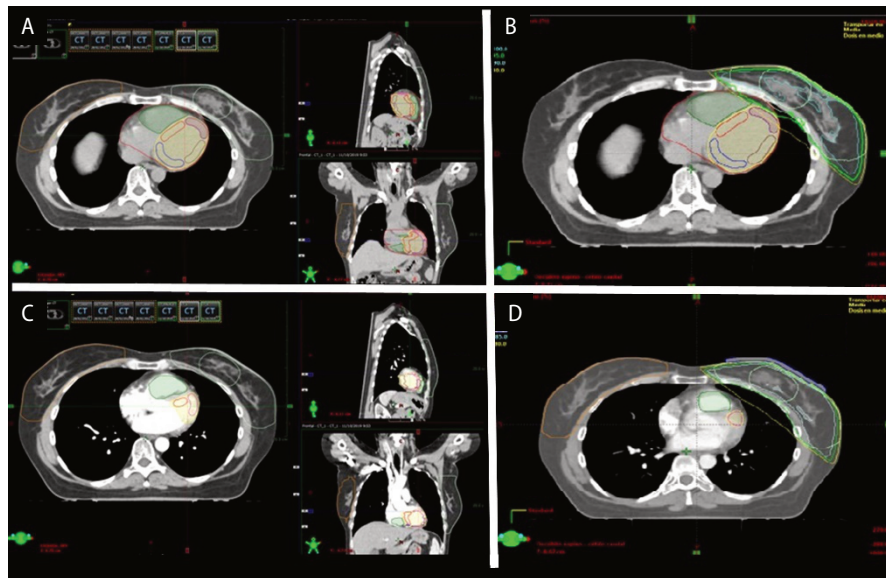


Figure 1. Computed tomography (CT) slices at the level of the target boost volume. Contours on the left column and isodose lines plus contours on the right column. CT-simulation under free-breathing (FB) conditions in the upper row and CT-simulation under deep inspiration breath-hold (DIBH) in the lower row. **A.** FB target and organs at risk (OARs) contours. Note the proximity of target volume to left ventricle anterior segment and right ventricle; **B.** FB treatment plan. Note that 80% isodose line (yellow) intersects with heart anterior wall, involving part of left ventricle anterior segment and right ventricle; **C.** DIBH target and OARs contours. Note the distance between target volume and left ventricle anterior segment and right ventricle due to pulmonary expansion. Multiplanar reconstruction (sagittal and coronal planes) show the diaphragm flattening and heart elongation due to DIBH. **D.** DIBH treatment plan. Note that 80% isodose line (yellow) does not intersect with heart anterior wall, sparing from high doses the left ventricle anterior segment and right ventricle

parameters corroborate the heart dose preservation with DIBH: Median V_{10} and V_{20} under FB were 3.9% and 2.3%, versus 1.1% and 0.5% under DIBH conditions ($p \leq 0.001$ for both comparisons). Figure 1 shows a demonstrative case highlighting the dosimetric benefit obtained from the DIBH technique.

Median D_{mean} to the LVs were 2.1 Gy for DIBH and 3.8 Gy for FB conditions ($p < 0.001$). Respective values for the right ventricles were 1.2 Gy under DIBH and 1.7 Gy for FB ($p < 0.001$). Median V_{20} for LVs was 0.3% under DIBH conditions, and 4.5% for FB conditions ($p < 0.001$). Median right ventricles V_{20} were 0.0% under both respiratory conditions.

LV segments doses

Median D_{mean} and V_{20} values for LV apical, anterior, septal, lateral, and inferior LV segments under DIBH and FB conditions are displayed in Table 3. Median doses were significantly reduced under DIBH conditions for every segment. V_{20} values were negligible in lateral, septal and posterior segments whatever the respiratory conditions, but for apical and anterior segments the V_{20} values were significantly reduced under DIBH condition.

Discussion

Two recent meta-analyses compared the heart dose, left lung dose, LAD coronary artery dose, and target coverage in 1019–3599 patients from 12–41 observational studies, respectively [6, 7]. Different respiratory monitoring devices were used in those studies: a belt in one study, real time surface tracking system in two studies, real time position management system in four studies, and active-breathing coordinator in five studies [6]. The combined analysis showed that there was no significant difference in target volumes coverage (D_{mean} and V_{95}) between the two groups [6]. Using the methods described in the present series, no difference in target coverage was observed.

The lung volume expansion under DIBH conditions is substantial, observing a mean volume difference of 1,638 mL for the whole lung, and 773 mL for the left lung. This volume expansion conditioned a significant decrease in the fraction of irradiated lung volume: a relative mean reduction of 9% for V_{20} , and 7% for V_{10} and V_5 . The values analyzed in the meta-analysis (left lung D_{mean} , V_{20} , V_{10}

and V5) were quite similar to the ones observed in the present study [6, 7]. Seven studies reported left-lung V20 values under DIBH conditions, resulting in a weighted mean of 11.6%, similar to the 12.1% observed in the present series [6]. For the V5 value, we observed 27.2% while a weighted mean value of 23.4% from six studies was reported in the Lai J. et al. meta-analysis [6]. The lung beneficial effect derived from the DIBH technique is not only related to total lung volume increment, but also to reduction in tissue density and, therefore, reduction of lung tissue mass in the treated volume underestimated through the dose-volume relationships the real sparing of lung parenchyma.

Few DIBH studies have reported a comparison between treatment techniques and lung dosimetric parameters. Zhao-Feng et al. [25] reported ipsilateral lung V20 d = -2.11% with 3DCRT and d = -1.29% with IMRT. As the patients in the present series were treated with IMRT, it is not surprising to obtain only small improvements for ipsilateral lung dosimetric parameters.

The coronary arteries integrity is essential to maintain the cardiac function. The artery more heavily damaged after breast irradiation is the LAD coronary artery [22]. According QUANTEC guidelines, the risk of radiation induced cardiac death at 10 years appears to be very low if MHD is < 3.3 Gy and maximum LAD dose is < 45.4 Gy [3]. Therefore, dose preservation on this vessel is of the highest importance. Under DIBH conditions, the radiation dose was dramatically diminished on LAD coronary artery in comparison with FB conditions, with relative reductions in D_{\max} , $D_{\text{quasi-max}}$ and V_{20} of 29%, 44%, and 93%, respectively. The Lai J. et al. meta-analysis showed a significant reduction in LAD coronary artery D_{mean} and D_{\max} [6]. Four studies included in the metanalysis reported mean LAD D_{\max} between 29.8–41.9 Gy under FB conditions versus 15.5–21.96 Gy under DIBH conditions. Corresponding figures in the present series were 36.2 Gy for FB and 24.4 Gy for DIBH. The data from 27 studies involving 2146 patients in Lu Y. et al. metanalysis demonstrated that the LAD dose (D_{mean} and D_{\max}) of the DIBH group was significantly lower than that of the FB group [7].

The heart volume difference was small (27 mL, about 5%), but statistically significant. It could be related to physiological factors or it could be just a contouring artefact. The DIBH heart compres-

sion effect has been reported previously [6]. As the dosimetric results are expressed in relative values, the small absolute volume difference does not deserve special consideration in the analysis. Dose to the heart as a whole organ and to the LV were significantly reduced under DIBH conditions. A reduction of 1.2 Gy in MHD, as observed in the present study, would represent a risk reduction of 9% for major coronary events according Darby's rule [1]. Based on more recent evidence, where the authors showed an increment of cumulative incidence of acute coronary events by 16.5% per Gy within 9 years of RT, a risk reduction of 20% for acute coronary events could be expected [22]. A recent study has shown that LAD- D_{mean} and MHD strongly correlated with coronary damage on computed tomographic angiography, with a 21% higher incidence of disease in the LAD per Gy for LAD- D_{mean} and a 95% higher incidence of disease in the LAD per Gy for MHD [23]. Therefore, a reduction of 1.2 Gy in MHD, as observed in the present study, would be followed by a substantial risk reduction in radiologically visible coronary disease.

It is under investigation which dose-distribution parameters, other than MHD and LAD dose, are good predictors for heart toxicity. The LV is the most exposed cardiac chamber during left-sided breast cancer 3D radiation therapy, with mean D_{mean} of 4.8 Gy according to Naimi et al. [10]. Similar D_{mean} value was obtained in the present study with IMRT under free-breathing conditions (mean D_{mean} of 4.5 Gy), but it was reduced to 2.5 Gy under DIBH conditions.

Zureick et al. have recently shown that increased LAD D_{mean} , LAD D_{\max} , and MHD were associated with increased risk of any cardiac event and a major cardiac event [24]. Van der Bogaard et al. showed that the volume of the LV receiving 5 Gy ($LV-V_{5\text{Gy}}$) was the most important prognostic dose-volume parameter, but only the four cardiac cavities were contoured in their study [26]. They chose the $LV-V_5$ parameter because heart- V_5 had been widely used in many other recent reports. The typical radiotherapy heart isodose map shows a very heterogeneous dose deposits in the LV, being the anterior and apical segments, the ones that receive higher doses. The subsegmental dosimetry in the present series showed that, in FB conditions, only the LV apex and anterior segments received a median dose larger than 5 Gy. Precisely, those segments

were the zones where DIBH reduced more intensely the radiation dose.

Conclusion

Demonstration of reduced doses to the left lung and cardiac structures with voluntary DIBH under spirometric control justifies the adoption of this technique as a standard method for left sided breast adjuvant irradiation because of its excellent dosimetric performance. For optimal heart sparing, LAD, LV and its apical/anterior segments should be considered as separate organs at risk.

Conflict of interest

Authors declare no conflict of interests.

Funding

Gerencia Regional de Salud de Castilla y León, GRS 1871/A/18.

References

1. Darby SC, Ewertz M, McGale P, et al. Risk of ischemic heart disease in women after radiotherapy for breast cancer. *N Engl J Med*. 2013; 368(11): 987–998, doi: [10.1056/NEJMoa1209825](https://doi.org/10.1056/NEJMoa1209825), indexed in Pubmed: [23484825](https://pubmed.ncbi.nlm.nih.gov/23484825/).
2. Erratum to: 2022 ESC Guidelines on cardio-oncology developed in collaboration with the European Hematology Association (EHA), the European Society for Therapeutic Radiology and Oncology (ESTRO) and the International Cardio-Oncology Society (IC-OS): Developed by the task force on cardio-oncology of the European Society of Cardiology (ESC). *Eur Heart J*. 2023; 44(18): 1621, doi: [10.1093/eurheartj/ehad196](https://doi.org/10.1093/eurheartj/ehad196), indexed in Pubmed: [36952225](https://pubmed.ncbi.nlm.nih.gov/36952225/).
3. Beaton L, Bergman A, Nichol A, et al. Cardiac death after breast radiotherapy and the QUANTEC cardiac guidelines. *Clin Transl Radiat Oncol*. 2019; 19: 39–45, doi: [10.1016/j.ctro.2019.08.001](https://doi.org/10.1016/j.ctro.2019.08.001), indexed in Pubmed: [31485490](https://pubmed.ncbi.nlm.nih.gov/31485490/).
4. Stowe HB, Andruska ND, Reynoso F, et al. Heart Sparing Radiotherapy Techniques in Breast Cancer: A Focus on Deep Inspiration Breath Hold. *Breast Cancer (Dove Med Press)*. 2022; 14: 175–186, doi: [10.2147/BCTT.S282799](https://doi.org/10.2147/BCTT.S282799), indexed in Pubmed: [35899145](https://pubmed.ncbi.nlm.nih.gov/35899145/).
5. Hanania AN, Mainwaring W, Ghebre YT, et al. Radiation-Induced Lung Injury: Assessment and Management. *Chest*. 2019; 156(1): 150–162, doi: [10.1016/j.chest.2019.03.033](https://doi.org/10.1016/j.chest.2019.03.033), indexed in Pubmed: [30998908](https://pubmed.ncbi.nlm.nih.gov/30998908/).
6. Lai J, Hu S, Luo Y, et al. Meta-analysis of deep inspiration breath hold (DIBH) versus free breathing (FB) in postoperative radiotherapy for left-side breast cancer. *Breast Cancer*. 2020; 27(2): 299–307, doi: [10.1007/s12282-019-01023-9](https://doi.org/10.1007/s12282-019-01023-9), indexed in Pubmed: [31707586](https://pubmed.ncbi.nlm.nih.gov/31707586/).
7. Lu Y, Yang Di, Zhang X, et al. Comparison of Deep Inspiration Breath Hold Versus Free Breathing in Radiotherapy for Left Sided Breast Cancer. *Front Oncol*. 2022; 12: 845037, doi: [10.3389/fonc.2022.845037](https://doi.org/10.3389/fonc.2022.845037), indexed in Pubmed: [35530354](https://pubmed.ncbi.nlm.nih.gov/35530354/).
8. S Nair S, Devi VN, Sharan K, et al. A Dosimetric Study Comparing Different Radiotherapy Planning Techniques With and Without Deep Inspiratory Breath Hold for Breast Cancer. *Cancer Manag Res*. 2022; 14: 3581–3587, doi: [10.2147/CMAR.S381316](https://doi.org/10.2147/CMAR.S381316), indexed in Pubmed: [36601278](https://pubmed.ncbi.nlm.nih.gov/36601278/).
9. Salvestrini V, Iorio GC, Borghetti P, et al. The impact of modern radiotherapy on long-term cardiac sequelae in breast cancer survivor: a focus on deep inspiration breath-hold (DIBH) technique. *J Cancer Res Clin Oncol*. 2022; 148(2): 409–417, doi: [10.1007/s00432-021-03875-1](https://doi.org/10.1007/s00432-021-03875-1), indexed in Pubmed: [34853887](https://pubmed.ncbi.nlm.nih.gov/34853887/).
10. Naimi Z, Moujahed R, Neji H, et al. Cardiac substructures exposure in left-sided breast cancer radiotherapy: Is the mean heart dose a reliable predictor of cardiac toxicity? *Cancer Radiother*. 2021; 25(3): 229–236, doi: [10.1016/j.canrad.2020.09.003](https://doi.org/10.1016/j.canrad.2020.09.003), indexed in Pubmed: [33423965](https://pubmed.ncbi.nlm.nih.gov/33423965/).
11. Zhou R, Liao Z, Pan T, et al. Cardiac atlas development and validation for automatic segmentation of cardiac substructures. *Radiother Oncol*. 2017; 122(1): 66–71, doi: [10.1016/j.radonc.2016.11.016](https://doi.org/10.1016/j.radonc.2016.11.016), indexed in Pubmed: [27939201](https://pubmed.ncbi.nlm.nih.gov/27939201/).
12. Finnegan R, Dowling J, Koh ES, et al. Feasibility of multi-atlas cardiac segmentation from thoracic planning CT in a probabilistic framework. *Phys Med Biol*. 2019; 64(8): 085006, doi: [10.1088/1361-6560/ab0ea6](https://doi.org/10.1088/1361-6560/ab0ea6), indexed in Pubmed: [30856618](https://pubmed.ncbi.nlm.nih.gov/30856618/).
13. Morris ED, Ghanem AI, Pantelic MV, et al. Cardiac Substructure Segmentation and Dosimetry Using a Novel Hybrid Magnetic Resonance and Computed Tomography Cardiac Atlas. *Int J Radiat Oncol Biol Phys*. 2019; 103(4): 985–993, doi: [10.1016/j.ijrobp.2018.11.025](https://doi.org/10.1016/j.ijrobp.2018.11.025), indexed in Pubmed: [30468849](https://pubmed.ncbi.nlm.nih.gov/30468849/).
14. Kaderka R, Gillespie EF, Mundt RC, et al. Geometric and dosimetric evaluation of atlas based auto-segmentation of cardiac structures in breast cancer patients. *Radiother Oncol*. 2019; 131: 215–220, doi: [10.1016/j.radonc.2018.07.013](https://doi.org/10.1016/j.radonc.2018.07.013), indexed in Pubmed: [30107948](https://pubmed.ncbi.nlm.nih.gov/30107948/).
15. Luo Y, Xu Y, Liao Z, et al. Automatic segmentation of cardiac substructures from noncontrast CT images: accurate enough for dosimetric analysis? *Acta Oncol*. 2019; 58(1): 81–87, doi: [10.1080/0284186X.2018.1521985](https://doi.org/10.1080/0284186X.2018.1521985), indexed in Pubmed: [30306817](https://pubmed.ncbi.nlm.nih.gov/30306817/).
16. Duane F, Aznar MC, Bartlett F, et al. A cardiac contouring atlas for radiotherapy. *Radiother Oncol*. 2017; 122(3): 416–422, doi: [10.1016/j.radonc.2017.01.008](https://doi.org/10.1016/j.radonc.2017.01.008), indexed in Pubmed: [28233564](https://pubmed.ncbi.nlm.nih.gov/28233564/).
17. Loap P, Marzi LDe, Kirov K, et al. Development of Simplified Auto-Segmentable Functional Cardiac Atlas. *Pract Radiat Oncol*. 2022; 12(6): 533–538, doi: [10.1016/j.prrro.2022.02.004](https://doi.org/10.1016/j.prrro.2022.02.004).
18. Milo ML, Nyeng TB, Lorenzen EL, et al. Atlas-based auto-segmentation for delineating the heart and cardiac substructures in breast cancer radiation therapy. *Acta Oncol*. 2022; 61(2): 247–254, doi: [10.1080/0284186X.2021.1967445](https://doi.org/10.1080/0284186X.2021.1967445), indexed in Pubmed: [34427497](https://pubmed.ncbi.nlm.nih.gov/34427497/).
19. Spoor DS, Sijtsema NM, van den Bogaard VAB, et al. Validation of separate multi-atlases for auto segmentation of cardiac substructures in CT-scans acquired in deep inspiration breath hold and free breathing. *Radiother Oncol*. 2021; 163: 46–54, doi: [10.1016/j.radonc.2021.07.025](https://doi.org/10.1016/j.radonc.2021.07.025), indexed in Pubmed: [34343547](https://pubmed.ncbi.nlm.nih.gov/34343547/).

20. Loap P, Tkatchenko N, Kirova Y. Evaluation of a delineation software for cardiac atlas-based autosegmentation: An example of the use of artificial intelligence in modern radiotherapy. *Cancer Radiother.* 2020; 24(8): 826–833, doi: [10.1016/j.canrad.2020.04.012](https://doi.org/10.1016/j.canrad.2020.04.012), indexed in Pubmed: [33144062](https://pubmed.ncbi.nlm.nih.gov/33144062/).
21. Offersen BV, Boersma LJ, Kirkove C, et al. ESTRO consensus guideline on target volume delineation for elective radiation therapy of early stage breast cancer, version 1.1. *Radiother Oncol.* 2016; 118(1): 205–208, doi: [10.1016/j.radonc.2015.12.027](https://doi.org/10.1016/j.radonc.2015.12.027), indexed in Pubmed: [26791404](https://pubmed.ncbi.nlm.nih.gov/26791404/).
22. van den Bogaard VAB, Ta BDP, van der Schaaf A, et al. Validation and Modification of a Prediction Model for Acute Cardiac Events in Patients With Breast Cancer Treated With Radiotherapy Based on Three-Dimensional Dose Distributions to Cardiac Substructures. *J Clin Oncol.* 2017; 35(11): 1171–1178, doi: [10.1200/JCO.2016.69.8480](https://doi.org/10.1200/JCO.2016.69.8480), indexed in Pubmed: [28095159](https://pubmed.ncbi.nlm.nih.gov/28095159/).
23. Tagami T, Almahariq MF, Balanescu DV, et al. Usefulness of Coronary Computed Tomographic Angiography to Evaluate Coronary Artery Disease in Radiotherapy-Treated Breast Cancer Survivors. *Am J Cardiol.* 2021; 143: 14–20, doi: [10.1016/j.amjcard.2020.12.038](https://doi.org/10.1016/j.amjcard.2020.12.038), indexed in Pubmed: [33359199](https://pubmed.ncbi.nlm.nih.gov/33359199/).
24. Zhao F, Shen J, Lu Z, et al. Abdominal DIBH reduces the cardiac dose even further: a prospective analysis. *Radiat Oncol.* 2018; 13(1): 116, doi: [10.1186/s13014-018-1062-6](https://doi.org/10.1186/s13014-018-1062-6), indexed in Pubmed: [29929560](https://pubmed.ncbi.nlm.nih.gov/29929560/).
25. Zureick AH, Grzywacz VP, Almahariq MF, et al. Dose to the Left Anterior Descending Artery Correlates With Cardiac Events After Irradiation for Breast Cancer. *Int J Radiat Oncol Biol Phys.* 2022; 114(1): 130–139, doi: [10.1016/j.ijrobp.2022.04.019](https://doi.org/10.1016/j.ijrobp.2022.04.019), indexed in Pubmed: [35483540](https://pubmed.ncbi.nlm.nih.gov/35483540/).